

On the Estimation of Notch Fatigue Limits by Using the Theory of Critical Distances: L , a_0 and Open Notches

L. Susmel^{1,2}, D. Taylor², R. Tovo¹

Abstract: This paper investigates some theoretical aspects related to the use of the Theory of Critical Distances (TCD) when employed to estimate notch fatigue limits. The linear-elastic TCD takes as a starting point the hypothesis that notched components are in their fatigue limit condition when an effective stress, whose value depends on a characteristic length, equals the material plain fatigue limit. Such an idea can be formalised by following different strategies: either assuming that the effective stress depends only on the profile of the stress field damaging the fatigue process zone and the reference distance is a material property or assuming that, for a given material, the values of both critical stress and critical distance change as the geometrical feature weakening the component to be assessed changes. The accuracy of the above different formalisations of the TCD was systematically checked by using experimental data taken from the literature and generated by testing metallic samples containing different types of notches. This systematic validation allowed us to confirm that the simplest formalisation of the TCD, in which both critical distance and critical stress are material constants, is also the most accurate one, giving predictions falling within an error interval of about $\pm 20\%$. Subsequently, in order to better explore the peculiarities of the above formalisation of the TCD, its accuracy was also checked considering notches having large values of the opening angle. This type of notch represents an interesting testing ground for our theory because, when the opening angle becomes larger than about 90° , the profile of the linear elastic-stress in the fatigue process zone is

strongly influenced by such an angle. The comparison with the experimental data proved that the TCD formalisation based on the assumption that both critical distance and critical stress are material constants is successful also in assessing these particular geometrical features. The exercises summarised in the present paper allowed us to further confirm that the simplest formalisation of the TCD is a powerful engineering tool, allowing real components to be assessed with an adequate degree of safety by simply post-processing linear-elastic Finite Element (FE) models.

Keyword: Theory of Critical Distances, Notch fatigue limit, open notches.

Nomenclature

| | |
|---|---|
| r, θ | Polar coordinates |
| r_n | Notch root radius |
| D_{LM} | Critical distance to apply the Line Method |
| D_{PM} | Critical distance to apply the Point Method |
| D_{AM} | Critical distance to apply the Area Method |
| L | Material characteristic length |
| R | Load ratio ($R = \sigma_{\min}/\sigma_{\max}$) |
| θ | Angle locating the plane experiencing the maximum normal stress |
| $\sigma_\theta, \sigma_r, \tau_{r\theta}$ | Stress components referred to the adopted polar coordinates |
| ΔK_{th} | Range of the threshold value of the stress intensity factor |
| $\Delta \sigma_0$ | Range of the plain fatigue limit |
| $\Delta \sigma_{A,g}$ | Range of the nominal notch fatigue limit (referred to the gross area) |
| $\Delta \sigma_1$ | Range of the maximum principal stress |

¹ Department of Engineering, University of Ferrara, Via Saragat, 1 – 44100 Ferrara, Italy

² Department of Mechanical Engineering, Trinity College, Dublin 2, Ireland

$\Delta\sigma_{eff}$ Range of the effective stress
calculated according to the TCD

1 Introduction

At the beginning of the last century, Neuber (Neuber, 1936; Neuber, 1958) formalised the so-called Line Method (LM) to predict fatigue strength of notched mechanical components. In particular, he formed the hypothesis that the elastic-stress distributions close to the stress riser apices do not reach values as high as the ones calculated according to the continuum mechanics theory. Following this intuition, he suggested averaging the linear-elastic stress over materials units in order to calculate an effective stress suitable for quantifying fatigue damage in the presence of stress concentration phenomena. A few years later, Peterson (Peterson, 1959) simplified Neuber's idea even more by observing that the above effective stress could simply be calculated at a given distance from the apex of the stress concentrator (Point Method, PM). Finally, in recent years, the TCD was successfully reformulated by taking full advantage of some LEFM findings (Tanaka, 1983; Lazzarin, Tovo and Meneghetti, 1997; Taylor, 1999). In this scenario, the present paper attempts to investigate some peculiar aspects of the use of the TCD to predict notch fatigue limits. In particular, by using several experimental datasets taken from the literature, the accuracies of some formalisations of the TCD, devised by forming different initial hypotheses, were systematically compared, investigating also the TCD capability of assessing stress concentrators characterised by large values of the notch opening angle.

2 Different Formalisations of the TCD

The TCD postulates that notched components are in the fatigue limit condition when the effective stress, $\Delta\sigma_{eff}$, calculated using the linear-elastic stress field damaging the fatigue process zone, is equal to the material plain fatigue limit, $\Delta\sigma_0$. In more detail, and according to the most modern formalisations of the TCD, $\Delta\sigma_{eff}$ can be calculated variously, as follows (Fig. 1a):

$$\Delta\sigma_{eff} = \Delta\sigma_1(\theta = 0, r = D_{PM}) = \Delta\sigma_0 \quad (1)$$

$$\Delta\sigma_{eff} = \frac{1}{2D_{LM}} \int_0^{D_{LM}} \Delta\sigma_1(\theta = 0, r) dr = \Delta\sigma_0 \quad (2)$$

$$\Delta\sigma_{eff} = \frac{4}{\pi D_{AM}^2} \int_0^{-\pi/2} \int_0^{D_{AM}} \Delta\sigma_1(r, \theta) \cdot dr \cdot d\theta \cong \Delta\sigma_0 \quad (3)$$

Eq. (1) formalises the Point Method, PM (Tanaka, 1983; Taylor, 1999), Eq. (2) the Line Method, LM (Tanaka, 1983; Lazzarin, Tovo, Meneghetti, 1997; Taylor, 1999;) and, finally, Eq. (3) the so-called Area Method, AM (Taylor, 1999). In these equations D_{PM} , D_{LM} and D_{AM} are the critical lengths to be used to apply the PM, the LM and the AM, respectively.

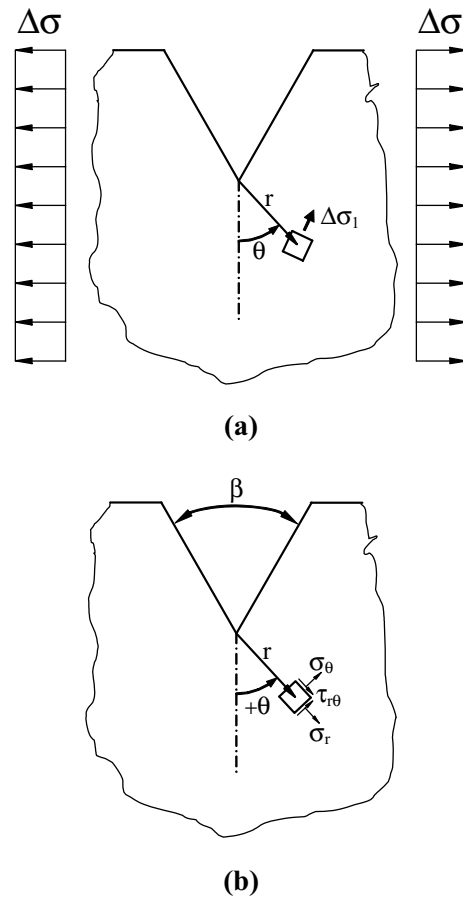


Figure 1: Definition of the local polar coordinates used to determine the linear-elastic stress fields damaging the fatigue process zone in notched specimens.

According to suggestions by Tanaka (Tanaka, 1983), Lazzarin and co-workers (Lazzarin, Tovo, Meneghetti, 1997) and Taylor (Taylor, 1999), these critical lengths take on the following values: $D_{PM} = L/2$, $D_{LM} = 2L$ and $D_{AM} = L$, where L is the material characteristic length, which is defined as (El Haddad, Smith, Topper, 1979):

$$L = \frac{1}{\pi} \left(\frac{\Delta K_{th}}{\Delta \sigma_0} \right)^2 \quad (4)$$

Here ΔK_{th} is the range of the threshold value of the stress intensity factor and $\Delta \sigma_0$ is the plain fatigue limit, both determined at the appropriate load ratio, R .

Previously, the accuracy of the above formalisations of the TCD was systematically checked, considering both standard notches (Taylor, Wang, 2000; Susmel, Taylor, 2003; Livieri, Tovo, 2004) and real components (Taylor, Bologna, Bel Knani, 2000): these investigations allowed us to prove that the TCD is successful in estimating notch fatigue limits, giving predictions falling within an error interval of about $\pm 20\%$. This raises the simple question: "Why does the TCD work?". Even though it is very difficult to answer this question coming to a definitive conclusion, we have noted that the TCD may work because it is capable of predicting the propagation (or non-propagation) of cracks initiating at the tip of the stress raiser and having length equal to $2L$ (Taylor, 2001). In other words, according to this idea, non-propagating cracks (NPCs) should have a length equal to $2L$ when initiated at the apex of crack-like notches. Though this justification is appealing, it does not explain the reason why the TCD is successful also in predicting fatigue limits of blunt notches (Taylor, 2001; Susmel, Taylor, 2003).

In any case, assuming that the TCD's accuracy is due to its capability of predicting NPCs' length, one may argue that, according to Yates and Brown's idea (Yates, Brown, 1987), the critical lengths in Eqs. (1), (2) and (3) are not related to L but to a_0 , which is defined as follows:

$$a_0 = \frac{1}{\pi} \left(\frac{\Delta K_{th}}{F \cdot \Delta \sigma_0} \right)^2 \quad (5)$$

Here F is the geometrical correction factor for the LEFM stress intensity factor, which depends on notch geometry and other factors, thus a_0 is not a material constant. If the maximum length of NPCs were correctly predicted by Eq. (5), then an alternative formulation of the TCD would use the following three critical distances: $D_{PM} = a_0/2$, $D_{LM} = 2a_0$ and $D_{AM} = a_0$. Now the question is: "Are the predictions made using a_0 more accurate than the ones obtained using L ?". In order to answer this question, in the next section the accuracy of these two different ways of using the TCD will be checked and compared by using experimental data taken from the literature.

Contrary to the PM formalisation discussed above, in 1997 Lazzarin, Tovo and Meneghetti argued that, in order to correctly apply such a predictive method, the range of the maximum principal stress at the point having coordinates $\theta=0$ and $r = L$ (see Fig. 1a) must be corrected by using an adimensional function depending on both L and the notch root radius, r_n . Their PM was defined then as (LTM-PM):

$$\Delta \sigma_{eff} = \Delta \sigma_1 (\theta = 0, r = L) \cdot f(r_n, L) = \Delta \sigma_0 \quad (6)$$

In order to obtain an explicit expression for function $f(r_n, L)$, Lazzarin and co-workers initially observed that when conventional notches are considered, and as long as the notch opening angle is lower than 90° , the maximum principal stress along the notch bisector can satisfactorily be described by using Glinka's equation (Glinka, Newport, 1987), that is, by assuming that the profile of the stress field in the vicinity of stress concentrators is mainly influenced by the tip radius, r_n . Therefore, if Glinka's analytical stress field is used together with Eq. (6), function $f(r_n, L)$ can be calibrated by considering the two extreme cases of a plain ($r_n = \infty$) and of a cracked component ($r_n=0$), obtaining the following expression for the LTM-PM:

$$\Delta \sigma_{eff} = \Delta \sigma_1 (\theta = 0, r = L) \frac{1 + \sqrt{2} \frac{L}{r_n}}{1 + \frac{L}{r_n}} = \Delta \sigma_0 \quad (7)$$

Thus, for these workers, the effective stress range depends on both the geometrical feature contained by the component to be assessed and the

material fatigue properties (through length L). In the next section, the selected data will be used also to discover what formalisation of the PM is the most accurate one.

To conclude, it is interesting to highlight that, in order to correctly define function $f(r_n, L)$ in Eq. (6), such an adimensional correction factor should be determined by using always analytical expressions suitable for accurately describing the linear-elastic stress field in the vicinity of the geometrical feature to be assessed. This aspect may limit in a way the use of such a formalisation of the PM when assessing real components having complex geometry, because, unfortunately, analytical solutions in close form are available only for standard notches.

3 Systematic Comparison Using Experimental Data

In order to answer the questions arising in the previous section, trying, at the same time, to express an objective verdict based on the experimental evidence, several data were selected from the technical literature. The summary of the experimental results considered in the present work are reported in Tables 1, 2 and 3. In particular, Table 1 summarises the fatigue properties of the investigated materials, whereas Tables 2 and 3 list the experimental fatigue limits generated by testing specimens of different materials and containing different geometrical features. It is worth mentioning that the considered notches were classified into blunt, short and sharp according to the rules proposed by Taylor (Taylor, 2001). The shape factors, F , were calculated by the Finite Element (FE) Method following the procedure already adopted by Atzori, Lazzarin and Meneghetti (Atzori, Lazzarin, Meneghetti, 2003). Finally, the linear-elastic stress fields damaging the fatigue process zone and needed to apply the TCD were determined by post-processing linear-elastic FE models done by using commercial software ANSYS®.

The above datasets were initially used to attempt to discover what formalisation of the TCD is the most accurate one when conventional notches having notch opening angle lower than 90° are

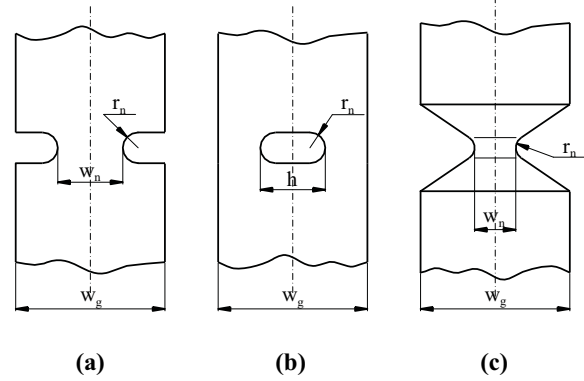


Figure 2: Geometries of the investigated notched specimens and definition of the adopted symbolism.

considered. Figures 3, 4 and 5 show the accuracy of the different formalisations of the TCD when the critical distance is assumed to be a function of either L or a_0 . In more detail, the above figures report three different charts: the plain fatigue limit, $\Delta\sigma_0$, vs. effective stress, $\Delta\sigma_{eff}$, diagrams obtained considering L (a) as well as a_0 (b) and the Probability Density Function vs. Error diagram (c). The latter diagram was reported to more easily compare the accuracy of the different formalisations of the TCD and it was built by assuming a normal distribution of the error. The error index was calculated as:

$$Error[\%] = \left(\frac{\Delta\sigma_{eff} - \Delta\sigma_0}{\Delta\sigma_0} \right) \cdot 100 \quad (8)$$

According to the above definition, the error index is equal to zero when predictions are exact, whereas when such an index takes on positive or negative values estimates are conservative or non-conservative, respectively.

Figures 3, 4 and 5 clearly prove that the L based TCD is much more accurate than the a_0 based critical distance method. In particular, it can be seen from the $\Delta\sigma_0$ vs. $\Delta\sigma_{eff}$ diagrams that the use of L to define the material characteristic length resulted in predictions falling mainly within an error interval of about $\pm 20\%$. Further, the Probability Density Function vs. Error diagrams of Figures 3, 4, and 5 show that, for the data considered in the present study, the lowest standard deviation value was obtained by applying the L based LM, even

Table 1: Fatigue properties of the investigated materials.

| Material | Ref. | R | $\Delta\sigma_0$ | ΔK_{th} |
|--------------|--|-----|------------------|-------------------------|
| | | | [MPa] | [MPa m ^{1/2}] |
| Mild Steel | Frost, 1957; Frost, 1959 | -1 | 420 | 12.8 |
| C45 | Nisitani, Endo, 1988 | -1 | 582 | 8.1 |
| C36 | Nisitani, Endo, 1988 | -1 | 446 | 7.1 |
| 6060-T6 | Luise, 2001 | 0.1 | 110 | 6.1 |
| AISI 304 | Harkegard, 1981 | -1 | 720 | 12.0 |
| EN-GJS-800-8 | Gasparini, Meneghetti 2002 | 0.1 | 440 | 8.1 |
| | | -1 | 155 | 15.9 |
| | | 0.1 | 99 | 11.2 |
| Grey Iron | Taylor et al., 1996 | 0.5 | 68 | 8.0 |
| | | 0.7 | 48 | 5.2 |
| AA356-T6 | Atzori et al., 2004 | -1 | 231 | 4.4 |
| Ni-Cr Steel | Frost, 1959 | -1 | 1000 | 12.8 |
| Steel 15313 | Lukas et al., 1986 | -1 | 440 | 12 |
| | | -1 | 326 | 12.4 |
| SM41B | Tanaka, Nakai, 1983; Tanaka, Akiniwa, 1987 | 0 | 274 | 8.4 |
| | | 0.4 | 244 | 6.4 |
| G40.11 | El Haddad, 1978 | -1 | 540 | 11.5 |
| FeP04 | Atzori et al., 2006 | 0.1 | 247 | 10.0 |
| HT 60 (1) | Usami, 1987 | 0 | 580 | 13.0 |
| SS41 | Kihara, Yoshii, 1991 | 0.1 | 231 | 6.4 |
| HT 60 (2) | Kihara, Yoshii, 1991 | 0.1 | 425 | 6.6 |

Table 2: Fatigue results generated by testing, under uniaxial loading, double edge notched plates (see Figure 2a for the specimen geometry as well as for the adopted symbolism).

| Material | w_n | w_g | r_n | β | F | Notch type | R | $\Delta\sigma_{A,g}$ |
|--------------|-------|-------|-------|---------|-------|------------|-----|----------------------|
| | [mm] | [mm] | [mm] | [°] | | | | [MPa] |
| Mild Steel | 53.34 | 63.5 | 0.1 | 55 | 1.12 | Sharp | -1 | 84.2 |
| | 53.34 | 63.5 | 0.25 | 55 | 1.12 | Sharp | -1 | 90.8 |
| | 53.34 | 63.5 | 0.51 | 55 | 1.12 | Sharp | -1 | 84.2 |
| | 53.34 | 63.5 | 1.27 | 55 | 1.12 | Sharp | -1 | 104.4 |
| | 53.34 | 63.5 | 7.62 | 55 | 1.12 | Blunt | -1 | 156.4 |
| 6060-T6 | 45 | 50 | 1.25 | 0 | 1.12 | Sharp | 0.1 | 55.0 |
| | 30 | 50 | 2 | 0 | 1.13 | Sharp | 0.1 | 31.7 |
| | 45 | 50 | 0.2 | 0 | 1.12 | Sharp | 0.1 | 47.6 |
| | 30 | 50 | 0.2 | 0 | 1.13 | Sharp | 0.1 | 25.4 |
| EN-GJS-800-8 | 19.2 | 20 | 0.04 | 90 | 1.126 | Sharp | 0.1 | 138.9 |
| | 18 | 20 | 0.1 | 90 | 1.13 | Sharp | 0.1 | 98.6 |

Table 3: Fatigue results generated by testing notched cylindrical bars (see Figure 2c for the specimen geometry as well as for the adopted symbolism).

| Material | w_n | w_g | r_n | β | F | Notch type | R | $\frac{\Delta\sigma_{A,g}}{[MPa]}$ | Load type* |
|-------------|-------|-------|-------|---------|-------|------------|-------|------------------------------------|------------|
| | [mm] | [mm] | [mm] | [°] | | | | | |
| Mild Steel | 33.02 | 43.18 | 0.05 | 55 | 1.308 | Sharp | -1 | 68.8 | AX |
| | 33.02 | 43.18 | 0.1 | 55 | 1.308 | Sharp | -1 | 70.0 | |
| | 33.02 | 43.18 | 0.13 | 55 | 1.308 | Sharp | -1 | 67.7 | |
| | 33.02 | 43.18 | 0.25 | 55 | 1.308 | Sharp | -1 | 69.6 | |
| | 33.02 | 43.18 | 0.64 | 55 | 1.308 | Sharp | -1 | 69.6 | |
| | 33.02 | 43.18 | 1.27 | 55 | 1.308 | Sharp | -1 | 77.0 | |
| | 33.02 | 43.18 | 5.08 | - | 1.308 | Blunt | -1 | 121.3 | |
| Ni-Cr Steel | 21.59 | 22.61 | 0.13 | 55 | 1.147 | Sharp | -1 | 236.0 | AX |
| | 32.84 | 43 | 0.05 | 55 | 1.308 | Sharp | -1 | 88.6 | |
| | 21.64 | 31.8 | 0.13 | 55 | 1.427 | Sharp | -1 | 96.6 | |
| C45 | 5 | 5.01 | 0.05 | 60 | 1.09 | Short | -1 | 546.7 | RB |
| | 5 | 5.01 | 0.02 | 60 | 1.09 | Short | -1 | 546.7 | |
| | 5 | 5.01 | 0.01 | 60 | 1.09 | Short | -1 | 556.7 | |
| | 5 | 5.02 | 0.05 | 60 | 1.09 | Short | -1 | 484.2 | |
| | 5 | 5.02 | 0.02 | 60 | 1.09 | Short | -1 | 494.0 | |
| | 5 | 5.02 | 0.01 | 60 | 1.09 | Short | -1 | 484.2 | |
| | 5 | 5.2 | 0.6 | 60 | 1.096 | Short | -1 | 373.4 | |
| | 5 | 5.2 | 0.3 | 60 | 1.096 | Short | -1 | 337.8 | |
| | 5 | 5.2 | 0.1 | 60 | 1.096 | Short | -1 | 320.3 | |
| | 5 | 5.2 | 0.05 | 60 | 1.096 | Short | -1 | 320.0 | |
| | 5 | 5.2 | 0.02 | 60 | 1.096 | Short | -1 | 320.0 | |
| | 5 | 6 | 0.6 | 60 | 1.239 | Blunt | -1 | 208.3 | |
| | 5 | 6 | 0.3 | 60 | 1.239 | Sharp | -1 | 173.6 | |
| | 5 | 6 | 0.1 | 60 | 1.239 | Sharp | -1 | 162.0 | |
| | 5 | 6 | 0.05 | 60 | 1.239 | Sharp | -1 | 162.0 | |
| | 5 | 6 | 0.02 | 60 | 1.239 | Sharp | -1 | 167.8 | |
| 5 | 6 | 0.01 | 60 | 1.239 | Sharp | -1 | 167.8 | | |
| C36 | 13 | 15 | 0.2 | 60 | 1.09 | Short | -1 | 288.5 | RB |
| | 13 | 14.4 | 0.2 | 60 | 1.09 | Short | -1 | 254.0 | |
| | 13 | 14 | 0.2 | 60 | 1.09 | Blunt | -1 | 202.6 | |
| | 13 | 13.6 | 0.2 | 60 | 1.14 | Blunt | -1 | 163.3 | |
| | 13 | 13.3 | 0.2 | 60 | 1.16 | Blunt | -1 | 136.9 | |
| | 13 | 13.2 | 0.2 | 60 | 1.193 | Blunt | -1 | 113.3 | |
| AISI 304 | 32.84 | 43 | 0.05 | 0 | 1.308 | Sharp | -1 | 72.3 | AX |
| Grey Iron | 23.64 | 30 | 0.3 | 90 | 1.28 | Sharp | -1 | 91.0 | AX |
| | 23.64 | 30 | 0.3 | 90 | 1.28 | Sharp | 0.1 | 60.0 | |
| | 23.64 | 30 | 0.3 | 90 | 1.28 | Sharp | 0.5 | 44.0 | |
| | 23.64 | 30 | 0.3 | 90 | 1.28 | Sharp | 0.7 | 32.0 | |
| AA356-T6 | 7.08 | 7.56 | 0.1 | 80 | 1.141 | Short | -1 | 114.8 | RB |
| | 7.78 | 9.04 | 0.18 | 59 | 1.201 | Sharp | -1 | 109.8 | |
| | 6.43 | 9.03 | 0.09 | 60 | 1.557 | Sharp | -1 | 44.8 | |
| | 6.18 | 11.98 | 0.08 | 68 | 2.78 | Sharp | -1 | 17.7 | |
| Steel 15313 | 4.94 | 5 | 0.03 | 0 | 1.13 | Short | -1 | 429.5 | AX |
| | 4.9 | 5 | 0.05 | 0 | 1.133 | Short | -1 | 403.4 | |
| | 4.86 | 5 | 0.07 | 0 | 1.138 | Short | -1 | 321.2 | |
| | 4.6 | 5 | 0.2 | 0 | 1.168 | Short | -1 | 237.0 | |
| | 4.2 | 5 | 0.4 | 0 | 1.229 | Short | -1 | 208.9 | |
| | 3.48 | 5 | 0.76 | 0 | 1.4 | Sharp | -1 | 155.0 | |

*AX = axial loading; RB = rotating bending

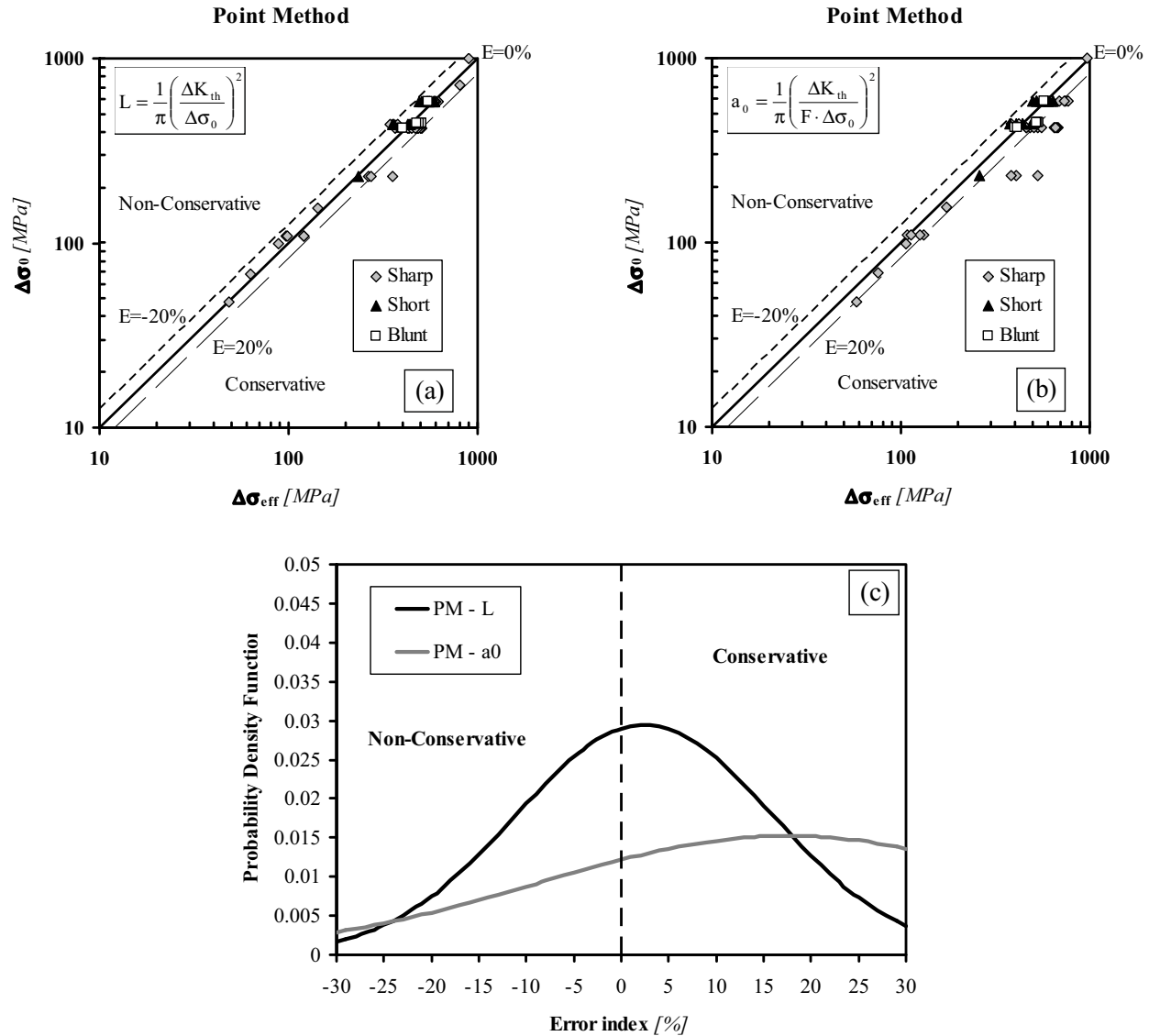


Figure 3: PM accuracy in predicting notch fatigue limits when the critical distance is assumed to be equal to L (a) and to a_0 (b); accuracy of the L based and the a_0 based PM in terms of Probability Density Function vs. Error index diagram (c).

if the peak of its error distribution was seen to be situated on the non-conservative side. On the contrary, the systematic application of the PM as well as of the AM, both applied by using L to define the material characteristic length, resulted in estimates characterised by slightly higher standard deviation values, with the peaks of the error distributions located in the conservative zone.

In order to further validate the accuracy of the L based PM, its error in estimating the selected notch fatigue limits was subsequently compared

to the one obtained by applying the PM (LTM-PM) devised by Lazzarin, Tovo and Meneghetti (Lazzarin, Tovo, Meneghetti, 1997) to the same set of data. As shortly said above, the main peculiarity of this predictive method is that the effective stress is assumed to be a complex function not only of the linear-elastic stress damaging the fatigue process zone, but also of both L and the notch root radius, r_n .

Observing that the two above formalisations of the PM take as a starting point the assumption

Table 4: Fatigue results generated by testing, under uniaxial loading, plates with central hole and having shape factor, F, equal to unity (see Figure 2b for the specimen geometry as well as for the adopted symbolism).

| Material | h | w_g | r_n | Notch type | R | $\Delta\sigma_{A,g}$ |
|-----------|------|-------|-------|------------|-------|----------------------|
| | [mm] | [mm] | [mm] | | | [MPa] |
| SM41B | 6 | 39 | 0.16 | Sharp | -1 | 95.3 |
| | 6 | 39 | 0.39 | Sharp | -1 | 104.0 |
| | 6 | 39 | 0.83 | Sharp | -1 | 95.3 |
| | 6 | 39 | 3 | Sharp | -1 | 128.3 |
| | 6 | 39 | 0.16 | Sharp | 0 | 63.3 |
| | 6 | 39 | 0.16 | Sharp | 0.4 | 73.0 |
| G40.11 | 0.4 | 70 | 0.2 | Short | -1 | 336.1 |
| | 0.96 | 70 | 0.48 | Short | -1 | 238.7 |
| | 9.6 | 70 | 4.8 | Blunt | -1 | 205.4 |
| SAE 1045 | 0.24 | 44.5 | 0.12 | Short | 0 | 325.0 |
| | 0.5 | 44.5 | 0.25 | Short | 0 | 308.0 |
| | 1.0 | 44.5 | 0.5 | Sharp | 0 | 270.0 |
| | 3.0 | 44.5 | 1.5 | Blunt | 0 | 212.0 |
| | 5.0 | 44.5 | 2.5 | Blunt | 0 | 209.0 |
| | 0.24 | 44.5 | 0.12 | Short | -1 | 357.0 |
| | 0.5 | 44.5 | 0.25 | Short | -1 | 306.0 |
| | 1.0 | 44.5 | 0.5 | Sharp | -1 | 273.0 |
| | 3.0 | 44.5 | 1.5 | Blunt | -1 | 231.0 |
| 5.0 | 44.5 | 2.5 | Blunt | -1 | 232.0 | |
| 2024-T351 | 0.24 | 44.5 | 0.12 | Short | 0 | 172.0 |
| | 0.5 | 44.5 | 0.25 | Short | 0 | 113.0 |
| | 1.0 | 44.5 | 0.5 | Sharp | 0 | 107.0 |
| | 3.0 | 44.5 | 1.5 | Blunt | 0 | 86.0 |
| | 0.24 | 44.5 | 0.12 | Short | -1 | 159.0 |
| | 0.5 | 44.5 | 0.25 | Short | -1 | 123.0 |
| | 1.0 | 44.5 | 0.5 | Sharp | -1 | 121.0 |
| 3.0 | 44.5 | 1.5 | Blunt | -1 | 84.0 | |

Table 5: Summary of the experimental results generated by testing open notches (see Figure 3 for the specimen geometry as well as for the adopted symbolism).

| Material | w_n | w_g | r_n | β | R | $\Delta\sigma_{A,g}$ | Geometry | |
|-----------|-------|-------|-------|---------|----------|----------------------|----------|---------|
| | [mm] | [mm] | [mm] | [°] | | [MPa] | | |
| FeP04 | 30 | 50 | 0.16 | 45 | 0.1 | 45.4 | Fig. 7a | |
| | 30 | 50 | 0.16 | 135 | 0.1 | 48.8 | | |
| | 30 | 50 | 0.16 | 160 | 0.1 | 87.2 | | |
| HT 60 (1) | 50 | 51 | 0.05 | 90 | 0 | 252.0 | Fig. 7a | |
| | 50 | 52 | 0.05 | 90 | 0 | 176.0 | | |
| | 50 | 60 | 0.05 | 90 | 0 | 90.0 | | |
| | 50 | 75 | 0.05 | 90 | 0 | 53.9 | | |
| | 50 | 51 | 0.05 | 135 | 0 | 257.8 | | |
| | 50 | 60 | 0.05 | 135 | 0 | 118.3 | | |
| | 50 | 75 | 0.05 | 135 | 0 | 75.3 | | |
| | 50 | 51 | 0.05 | 165 | 0 | 393.1 | | |
| | 50 | 52 | 0.05 | 165 | 0 | 375.0 | | |
| | 50 | 60 | 0.05 | 165 | 0 | 333.3 | | |
| | 50 | 75 | 0.05 | 165 | 0 | 215.3 | | |
| | 50 | - | 0.05 | 135 | 0 | 261.0 | | Fig. 7d |
| | 50 | - | 0.05 | 135 | 0 | 162.0 | | Fig. 7c |
| SS41 | 30 | 50 | 0.1 | 90 | 0.05 | 25.9 | Fig. 7a | |
| | 30 | 50 | 0.1 | 120 | 0.05 | 39.9 | Fig. 7b | |
| | 30 | 50 | 0.1 | 120 | 0.05 | 16.7 | Fig. 7b | |
| | 40 | - | 0.1 | 135 | 0.05 | 86.1 | Fig. 7c | |
| HT 60 (2) | 30 | 50 | 0.1 | 90 | 0.05 | 31.0 | Fig. 7a | |
| | 30 | 50 | 0.1 | 120 | 0.05 | 43.4 | | |
| | 30 | 50 | 0.1 | 120 | 0.05 | 17.2 | Fig. 7b | |
| | 40 | - | 0.1 | 135 | 0.05 | 130.0 | Fig. 7c | |
| | 40 | - | 0.1 | 150 | 0.05 | 144.0 | | |

Table 6: Values of constants λ_1 , λ_2 , χ_1 and χ_2 in Lazzarin and Tovo's equations.

| β [Rad] | λ_1 | χ_1 | λ_2 | χ_2 |
|------------------|-------------|----------|-------------|----------|
| 0 | 0.500 | 1.000 | 0.500 | 1.000 |
| $\pi/6$ | 0.501 | 1.071 | 0.598 | 0.921 |
| $\pi/4$ | 0.505 | 1.166 | 0.660 | 0.814 |
| $\pi/3$ | 0.512 | 1.312 | 0.731 | 0.658 |
| $\pi/2$ | 0.544 | 1.841 | 0.909 | 0.219 |
| $2\pi/3$ | 0.616 | 3.003 | 1.149 | -0.314 |
| $3\pi/4$ | 0.674 | 4.153 | 1.302 | -0.569 |
| $5\pi/6$ | 0.752 | 6.362 | 1.486 | 0.787 |

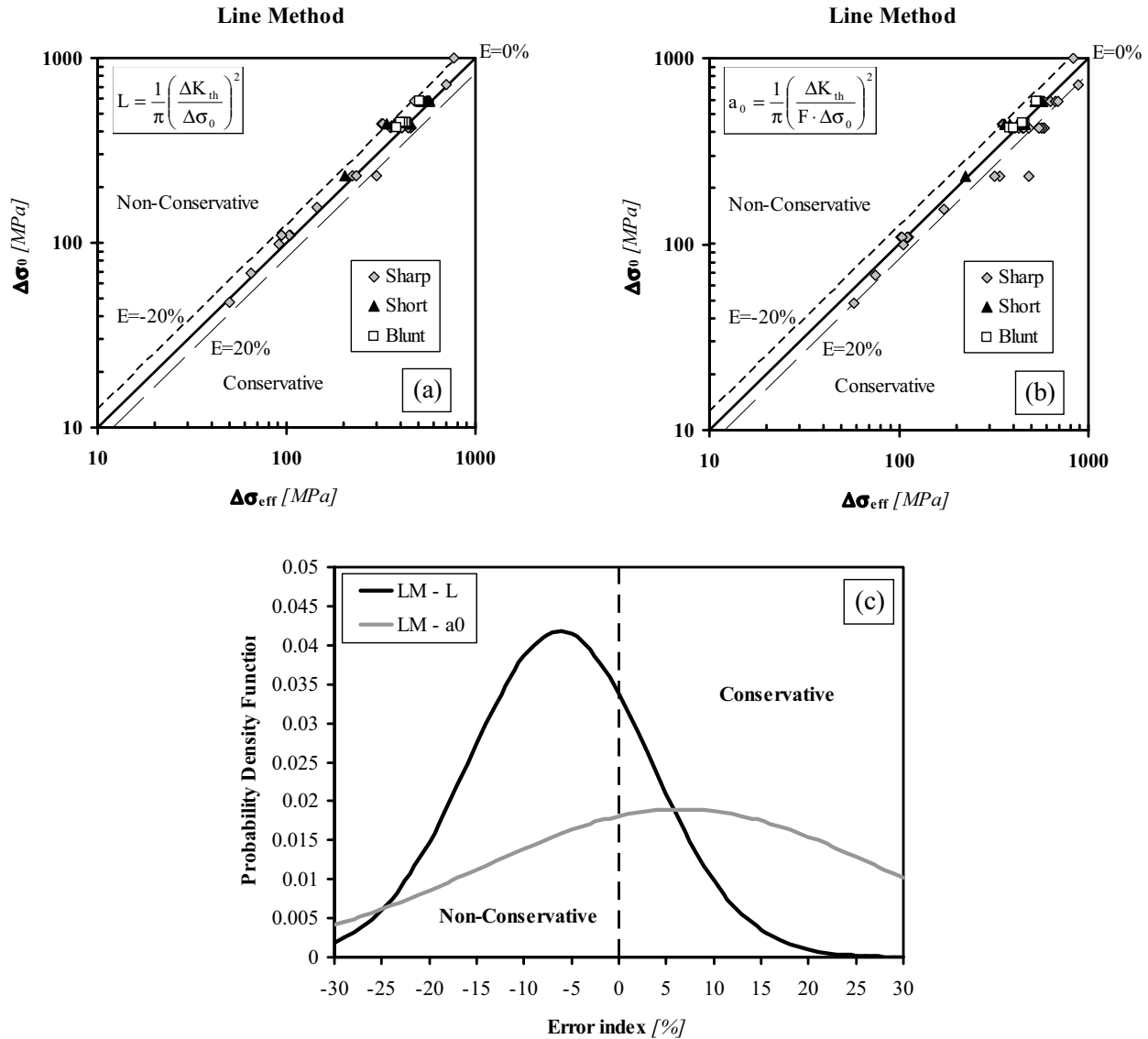


Figure 4: LM accuracy in predicting notch fatigue limits when the critical distance is assumed to be equal to L (a) and to a_0 (b); accuracy of the L based and the a_0 based LM in terms of Probability Density Function vs. Error index diagram (c).

that the characteristic length is a material property, their accuracies were compared not only considering the data summarised in Tables 2 and 3, and having $F > 1$, but also the results reported in Table 4. In particular, the latter sets of data were generated by testing plates, of different materials, with a central hole resulting in a shape factor, F , equal to unity. The $\Delta\sigma_0$ vs. $\Delta\sigma_{eff}$ diagrams reported in Figure 6 clearly show that the systematic application of the above two formalisations of the PM to the data listed in Tables 2, 3 and 4 practi-

cally resulted in the same accuracy level. This fact is also confirmed by the Probability Density Function vs. Error diagram of Figure 6c: the two error distributions were characterised by close values of the standard deviation. Moreover, it is interesting to highlight that the peak of the error distribution obtained by applying the LTM-PM was seen to be slightly non-conservative, i.e. the mean value was equal to -1.2% , whereas the error distribution of the L based PM had mean value equal to about 3% . According to the above considerations, and

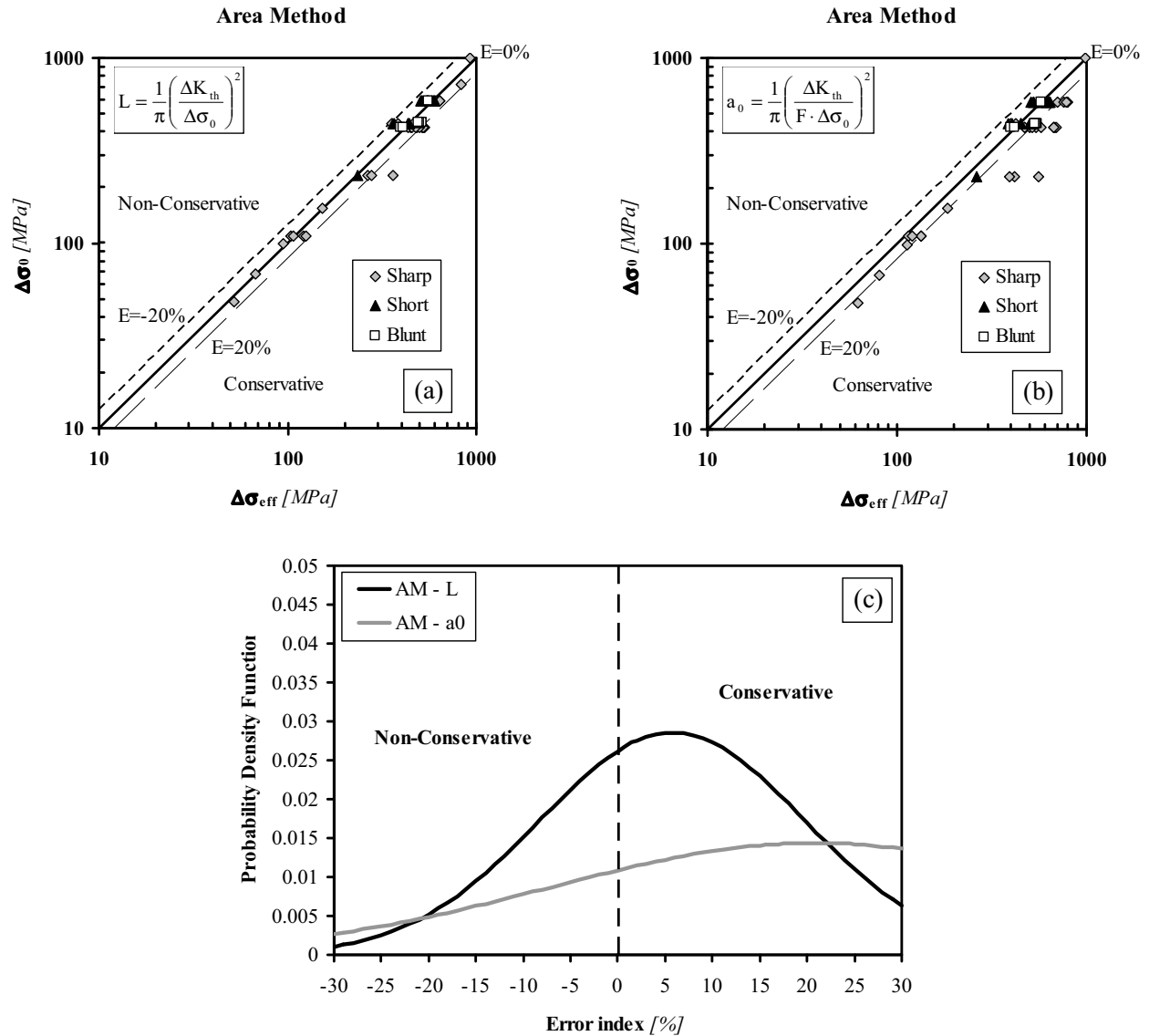


Figure 5: AM accuracy in predicting notch fatigue limits when the critical distance is assumed to be equal to L (a) and to a_0 (b); accuracy of the L based and the a_0 based AM in terms of Probability Density Function vs. Error index diagram (c).

remembering the intrinsic data scattering affecting fatigue results, it is possible to conclude saying that the use of both the L based PM and the LTM-PM results in the same accuracy level, even if the two approaches are based on different initial assumptions.

To conclude, it can be observed that the validation exercise summarised in the present section seems to strongly support the idea that the critical distance can be assumed to be a material constant, that is, unaffected by notch geometry. This fact

suggests that the L based TCD can be applied with confidence to real stress concentration features on components, which often have very complex geometry, because such a simple method allows real mechanical assemblies to always be assessed with an adequate degree of safety.

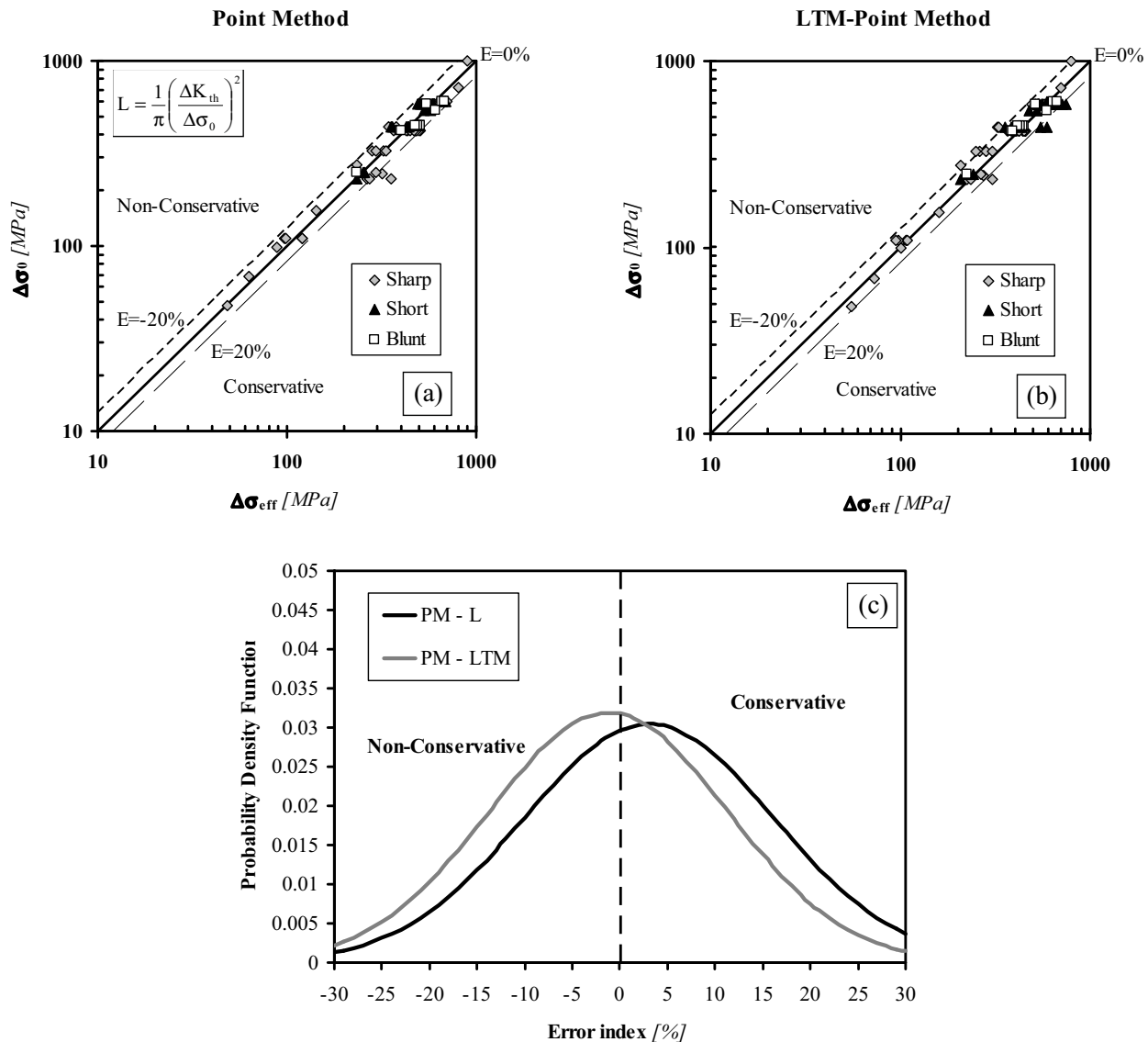


Figure 6: Accuracy of the L based PM (a) and Lazzarin, Tovo and Menghetti's PM (b) in predicting notch fatigue limits and resulting Probability Density Function vs. Error index diagram (c).

4 L Based TCD Accuracy in Predicting High-Cycle Fatigue Strength in the Presence of Open Notches

In light of the sound agreement between estimates and experimental results obtained by assuming that both critical distance and critical stress are material constants, such a formalisation of the TCD was subsequently attempted to be used to predict fatigue limits generated by testing notches having opening angles larger than 90° . The summary of the considered experimental results is reported in Table 5, whereas the geometries of the

investigated specimens are sketched in Figure 7.

In order to briefly review the peculiarities of the linear-elastic stress field distributions in the presence of open notches, consider the V-notched specimen of Figure 1b. According to the asymptotic solutions first formalised by Williams (Williams, 1959), Lazzarin and Tovo suggested describing the linear-elastic stress fields in the vicinity of sharp re-entrant corners by using the

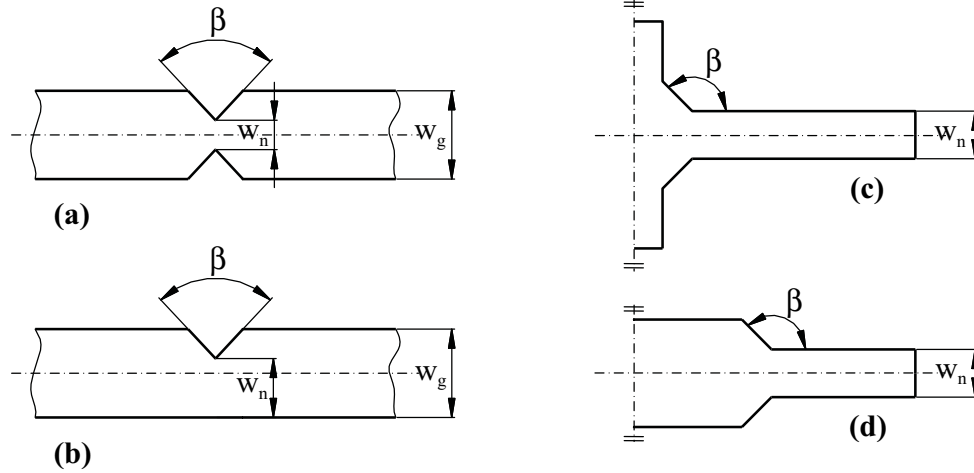


Figure 7: Geometries of the specimens weakened by open notches.

following equations (Lazzarin, Tovo, 1996):

$$\begin{aligned} \begin{Bmatrix} \sigma_\theta \\ \sigma_r \\ \tau_{r\theta} \end{Bmatrix}_{r_n=0} &= \frac{1}{\sqrt{2\pi}} \frac{r^{\lambda_1-1} K_1}{(1+\lambda_1) + \chi_1(1-\lambda_1)} \\ &\cdot \left[\begin{Bmatrix} (1+\lambda_1) \cos(1-\lambda_1)\theta \\ (3-\lambda_1) \cos(1-\lambda_1)\theta \\ (1-\lambda_1) \sin(1-\lambda_1)\theta \end{Bmatrix} \right. \\ &\quad \left. + \chi_1(1-\lambda_1) \begin{Bmatrix} \cos(1+\lambda_1)\theta \\ -\cos(1+\lambda_1)\theta \\ \sin(1+\lambda_1)\theta \end{Bmatrix} \right] \quad (9) \end{aligned}$$

$$\begin{aligned} \begin{Bmatrix} \sigma_\theta \\ \sigma_r \\ \tau_{r\theta} \end{Bmatrix}_{r_n=0} &= \frac{1}{\sqrt{2\pi}} \frac{r^{\lambda_2-1} K_2}{(1-\lambda_2) + \chi_2(1+\lambda_2)} \\ &\cdot \left[\begin{Bmatrix} -(1+\lambda_2) \sin(1-\lambda_2)\theta \\ -(3-\lambda_2) \sin(1-\lambda_2)\theta \\ (1-\lambda_2) \cos(1-\lambda_2)\theta \end{Bmatrix} \right. \\ &\quad \left. + \chi_2(1+\lambda_2) \begin{Bmatrix} -\sin(1+\lambda_2)\theta \\ \sin(1+\lambda_2)\theta \\ \cos(1+\lambda_2)\theta \end{Bmatrix} \right] \quad (10) \end{aligned}$$

In the above relationships, K_1 and K_2 are the Notch-Stress Intensity Factors (N-SIF) to be determined according to the definition proposed by Gross and Mandelson (Gross, Mendelson, 1972), whereas, as clearly shown by Table 6, constants λ_1 , λ_2 , χ_1 and χ_2 depend on the notch opening angle value, β . The above equations can also be

used in the presence of finite notch root radii, provided that they are rewritten as follows (Lazzarin, Tovo, 1996):

$$\begin{aligned} \begin{Bmatrix} \sigma_\theta \\ \sigma_r \\ \tau_{r\theta} \end{Bmatrix}_{r_n \neq 0} &= \begin{Bmatrix} \sigma_\theta \\ \sigma_r \\ \tau_{r\theta} \end{Bmatrix}_{r_n=0} + \frac{1}{\sqrt{2\pi}} \frac{K_1}{r_0^{1-\lambda_1}} \left(\frac{r}{r_0} \right)^{\mu_1-1} \\ &\frac{(3-\lambda_1) - \chi_1(1-\lambda_1)}{(1+\lambda_1) + \chi_1(1-\lambda_1)} \begin{Bmatrix} \cos(1+\mu_1)\theta \\ -\cos(1+\mu_1)\theta \\ \sin(1+\mu_1)\theta \end{Bmatrix} \quad (11) \end{aligned}$$

$$\begin{aligned} \begin{Bmatrix} \sigma_\theta \\ \sigma_r \\ \tau_{r\theta} \end{Bmatrix}_{r_n \neq 0} &= \begin{Bmatrix} \sigma_\theta \\ \sigma_r \\ \tau_{r\theta} \end{Bmatrix}_{r_n=0} + \frac{1}{\sqrt{2\pi}} \frac{K_2}{r_0^{1-\lambda_2}} \left(\frac{r}{r_0} \right)^{\mu_2-1} \\ &\begin{Bmatrix} \sin(1+\mu_2)\theta \\ -\sin(1+\mu_2)\theta \\ -\cos(1+\mu_2)\theta \end{Bmatrix} \quad (12) \end{aligned}$$

where constants μ_1 and μ_2 depend again on the opening angle value, whereas distance r_0 is a function of the notch root radius value, r_n (Lazzarin, Tovo, 1996).

Equations (9) and (10), together with Table 6, clearly show that the opening angle value strongly affects the stress distribution ahead of lateral V-notches and it holds true especially when notch opening angles become larger than about 100° . In other words, the notch opening angle is an important geometrical parameter to be considered, because, as it varies, the degree of singularity

of the stress field itself changes. Such an influence is clearly shown by the stress-distance curves sketched in Figure 8 and obtained by considering the samples tested by Atzori, Lazzarin and Meneghetti (Atzori, Lazzarin, Meneghetti, 2006). In more detail, the above curves refer to double edge V-notched specimens (Fig. 7a) subjected to a gross nominal tensile stress equal to 100 MPa and characterised by three different values of the notch opening angle: 45°, 135° and 160°. Figure 8 clearly shows that, given the geometry and the applied loading, the stress gradient in the vicinity of the notch tip decreases as the notch opening angle increases.

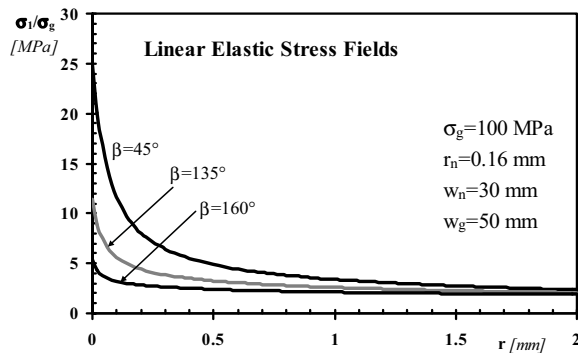


Figure 8: Opening angle influence on the maximum linear-elastic stress distribution in a V-notched plate loaded in tension (see Fig. 7a for the specimen geometry).

The above considerations should make it evident that open notches definitely represent an interesting and important testing ground to further check the accuracy and reliability of the TCD in estimating notch fatigue limits. Our theory was then applied to the experimental results summarised in Table 5. Again the stress fields damaging the fatigue process zone were determined by using ANSYS® code and the TCD was applied in terms of maximum principal stress range. Figure 9 reports the $\Delta\sigma_0$ vs. $\Delta\sigma_{eff}$ charts obtained by applying the L Based TCD in terms of both the PM (Fig. 9a), the LM (Fig. 9b) and the AM (Fig. 9c): again such a formalisation of the TCD proved to be highly accurate, giving predictions falling within an error interval of $\pm 20\%$, and this held true independently of notch opening angle value.

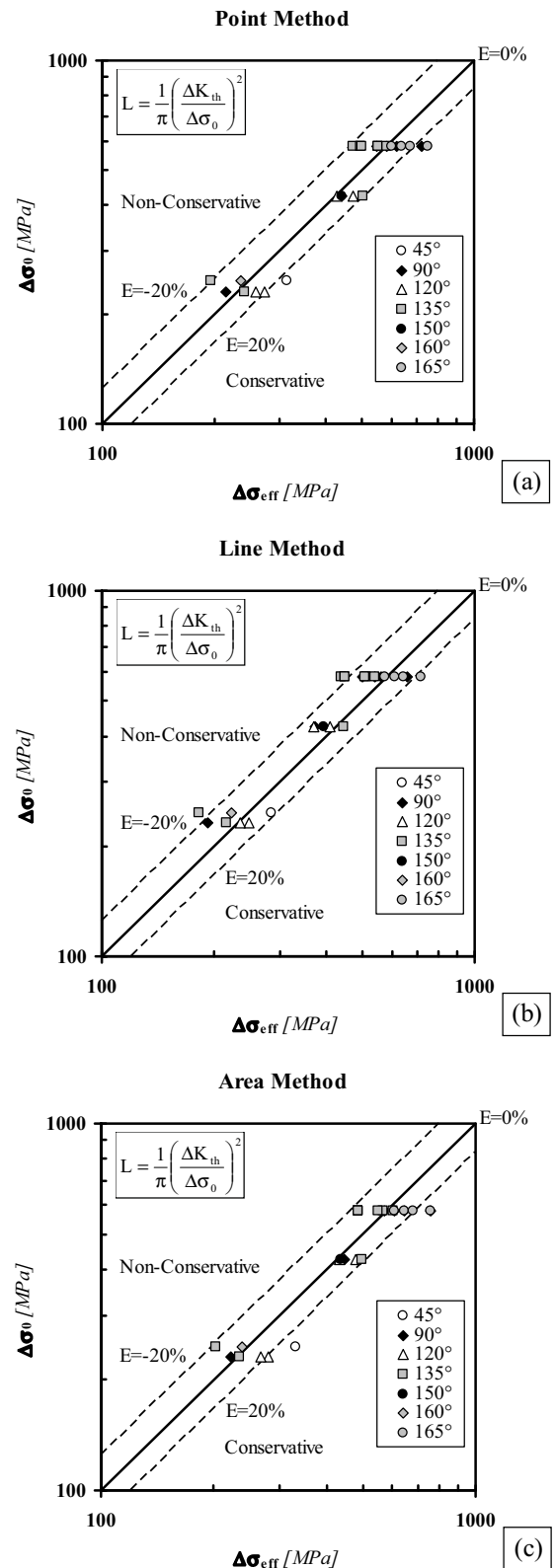


Figure 9: L based TCD accuracy in predicting fatigue limits of specimens weakened by open notches.

5 Discussion

This paper is concerned with the accuracy of the most modern formalisations of the TCD. In particular two different ways of calibrating such a theory were considered: either assuming that the effective stress depends only on the linear-elastic stress field damaging the fatigue process zone and the reference critical distance is a material property or taking as a starting point the idea that, for a given material, the value of either the effective stress or the critical distance changes as the geometrical feature contained by the component to be assessed changes.

The systematic comparison between the estimates obtained by using L to determine the critical length to those done by using a_0 (whose value depends, through shape factor F , not only on the material fatigue properties but also on the geometry as well as on the applied loading type) proved that the L Based TCD is the most accurate one: the use of L along with both the PM, the LM and the AM was seen to result in estimates falling within an error interval of about $\pm 20\%$, and it held true independently of geometrical feature, material and applied loading type.

Subsequently, the accuracy of the L Based PM was compared to the one of the PM (LTM-PM) devised by Lazzarin, Tovo and Meneghetti (Lazzarin, Tovo, Meneghetti, 1997). The main peculiarity of the latter approach is that the effective stress is assumed to be a complex function of both the linear-elastic stress field damaging the material in the vicinity of the notch tip, the geometrical feature (through the notch root radius) and the material characteristic length, L . The comparison based on several datasets taken from the literature allowed us to prove that the systematic use of both the L Based PM and the LTM-PM practically results in the same accuracy level.

As to the way the LTM-PM works, it has to be said that such an approach was applied to the selected data in the explicit form given by Lazzarin, Tovo and Meneghetti and based on the use of Glinka's equation to describe the linear elastic stress field damaging the fatigue process zone. As highlighted by the above authors, in the pres-

ence of particular geometrical features, other analytical solutions should be considered to properly describe the profile of the stress-distance curve needed to calibrate the method itself. This remark should make it evident that the use of other analytical solutions capable of better describing the stress fields in the vicinity of the investigated notches may have resulted in a higher accuracy level. In any case, it has to be said also that this aspect may limit in a way the use of such a formalisation of the PM, especially when real components having complex geometry are involved, because analytical solutions in close form are available only for standard notches. Certainly, more work deserves to be done in this area in order to better explore all the peculiarities of the PM as devised by Lazzarin and co-workers.

In light of the sound estimates obtained by applying the L Based TCD, we subsequently investigated its accuracy in predicting high-cycle fatigue strength of metallic specimens weakened by open notches, i.e. by notches having opening angle larger than 90° . As shortly said above, this kind of geometrical features represents a very interesting testing ground for our theory, because, for a given geometry, the opening angle value strongly affects the profile of the stress-distance curve needed to apply the TCD (and it holds true especially in the presence of notch opening angles larger than 90°). The systematic validation done by considering results generated by testing open notches weakening specimens of different metallic materials proved that the L Based TCD is capable of accurate predictions also when applied to specimens containing this particular type of geometrical feature, giving predictions again falling within an error interval of about $\pm 20\%$. In this scenario, it is also worth mentioning that Atzori, Lazzarin and Meneghetti came to a similar conclusion when validating their elegant approach ad hoc devised to assess open notches (Atzori, Lazzarin, Meneghetti, 2005). It has to be said also that the capability of the TCD in correctly estimating fatigue damage due to open notches was not surprising at all: such an approach was already seen to be very successful in predicting high-cycle fatigue strength of welded joints, that is, in the presence

of opening angles equal to about 135° (Taylor, Barret, Lucano, 2002; Crupi, Crupi, Guglielmino, Taylor, 2005).

As to the constancy of the material characteristic length, it is interesting to highlight here that, strictly speaking, for a given material, its experimental value is seen to change as the degree of multi-axiality of the linear-elastic stress field damaging the fatigue process zone changes. For instance, by reanalysing a large amount of experimental results it was proved that, in the high-cycle fatigue regime, the critical distance under torsion is different to its value determined under uniaxial fatigue loading (Susmel, Taylor, 2006). Fortunately, it was also seen that the TCD can efficiently be used to estimate notch torsional fatigue limits by simply keeping L constant and equal to its value determined under uniaxial fatigue loading: such an engineering assumption allows the TCD to be applied to torsional situations by calibrating it through pieces of experimental information generated, according to the pertinent standard codes, by using conventional uniaxial testing equipments. Besides, the fact that L can be assumed to be constant independently of the degree of multi-axiality of the assessed stress field results also in the fact that the TCD can be used to estimate notch fatigue limits independently of the complexity of the applied loading path, provided that it is used in conjunction with a suitable multi-axial fatigue criterion (Susmel, Taylor, 2003; Susmel, 2004; Susmel, Taylor, 2006). Another aspect of the problem which deserves to be mentioned here is the fact that L was seen to increase as the number of cycles to failure, N_f , increases (Susmel, Taylor, 2007). Even if the above experimental evidence can easily be taken into account to successfully extend the use of our theory down to the medium-cycle fatigue regime, it is worth noticing that this fact may result in further complications when attempting to use the TCD in the presence of random fatigue loading. These considerations should make it evident that more work is needed to be done in this area to formalise a sound procedure suitable for using the TCD to perform the fatigue assessment of notched components experiencing variable amplitude loading.

To conclude, it is interesting to observe that, by comparing the linear-elastic stress fields due to different geometrical features, Atzori, Lazzarin and Filippi (Atzori, Lazzarin, Filippi, 2001) recently argued that the differences between the PM and LM in predicting notch fatigue limits depend on both the notch geometry and the absolute value of the material characteristic length, L . The above conclusion, which is totally correct, was based on the systematic comparison of the linear elastic stress fields due to different notches, without considering any experimental notch fatigue limit. On the contrary, in the present work all the analyses we carried out were based on several experimental results generated by testing metallic specimens containing different geometrical features. Due to their nature, all the experimental values we considered were affected by two main variables: the intrinsic data scattering typical of fatigue results and the uncertainty in defining the actual notch geometry (especially in the presence of very small notch root radii). In light of this well known difficulties arising when dealing with practical problems (and it holds true especially when real components having complex geometry are involved) and supported by the highly accurate estimates obtained when applying the L Based TCD, we certainly feel so confident to suggest the use of such a theory also to assess real components in situations of practical interest: the main feature of the L based TCD is that it can directly be applied by post-processing linear-elastic FE results, without the need for correcting it to account for both the actual notch geometry and the absolute value of the material characteristic length, L .

6 Conclusions

1. The use of L to define the critical distance value was seen to result in more accurate results than the ones obtained by using short crack constant a_0 ;
2. The PM devised by Lazzarin, Tovo and Meneghetti was seen to be highly accurate, even if more work has to be done to make it suitable for being easily used to assess real components;

3. The L Based TCD proved to be very successful also in predicting high-cycle fatigue strength of metallic materials weakened by open notches.

References

- Atzori B., Lazzarin P., Filippi S.** (2001): Cracks and notches: analogies and differences of the relevant stress distributions and practical consequences in fatigue limit predictions. *Int J Fatigue* 23, pp. 355-362.
- Atzori B., Lazzarin P., Meneghetti G.** (2003): Fracture mechanics and notch sensitivity. *Fatigue Fract Engng Mater Struct* 26, pp. 257-267.
- Atzori B., Lazzarin P., Meneghetti G.** (2005): A unified treatment of the mode I fatigue limit of components containing notches or defects. *Int J Fracture* 133, pp. 61-87.
- Atzori, B., Lazzarin P., Meneghetti, G.** (2006): Estimation of fatigue limits of sharply notched components. In: *Proc. of Fatigue 2006*, Atlanta, Georgia, USA.
- Atzori, B., Meneghetti, G., Susmel, L.** (2004): Fatigue behaviour of AA356-T6 aluminium cast alloy weakened by cracks and notches. *Eng Frac Mech* 71, pp. 759-768.
- Crupi, G., Crupi, V., Guglielmino, E., Taylor, D.** (2005): Fatigue assessment of welded joints using critical distance and other methods. *Eng Fail Anal* 12, pp. 129-142.
- El Haddad, M. H.** (1978): A study of the growth of short fatigue cracks based on fracture mechanics. *Ph. D. Thesis*, University of Waterloo, Waterloo, Ontario, 1978.
- El Haddad, M. H., Smith, K. N., Topper, T. H.** (1979): Fatigue crack propagation of short cracks. *J Engng Mater Tech (Trans ASME)* 101, pp. 42-45.
- Frost, N. E.** (1959): A relation between the critical alternating propagation stress and crack length for mild steel. *Proc Inst Mech Engrs* 173, pp. 811-834.
- Frost, N. E.** (1957): Non-propagating cracks in V-notched specimens subjected to fatigue loading. *Aeronaut. Quart.* VIII, pp. 1-20.
- Gasparini, E., Meneghetti G.** (2002): Una banca dati sul comportamento a fatica delle ghise sferoidali austemperate. *La Metallurgia Italiana* 3, pp. 29-35 (in Italian).
- Glinka, G., Newport, A.** (1987): Universal features of elastic notch-tip stress fields. *Int J Fatigue* 9, pp. 143-150.
- Gross R., Mendelson A.** (1972): Plane elasto-static analysis of V-notched plates. *Int J Fracture Mechanics* 8, pp. 267-276.
- Harkegard G.** (1981): An effective stress intensity factor and the determination of the notched fatigue limit. In: *Fatigue Thresholds: Fundamentals and Engineering Applications*, Vol. II, Edited by J. Backlund, A. F. Blom and C. J. Beevers, Chameleon Press Ltd, London, pp. 867-879.
- Kihara, S., Yoshii, A.** (1991): A strength evaluation method of a sharply notched structure by a new parameter, the equivalent stress intensity factor. *JSME* 34, pp. 70-75.
- Lazzarin P., Tovo R.** (1996): A unified approach to the evaluation of linear elastic stress fields in the neighbourhood of cracks and notches. *Int J Fracture* 78, pp. 3-19.
- Lazzarin, P., Tovo, R., Meneghetti, G.** (1997): Fatigue crack initiation and propagation phases near notches in metals with low notch sensitivity. *Int. J Fatigue* 19, pp. 647-657.
- Livieri, P., Tovo, R.** (2004): Fatigue limit evaluation of notches, small cracks and defects: an engineering approach. *Fatigue Fract Engng Mater Struct* 27, pp. 1037-1049.
- Luise, M.** (2001): Caratterizzazione a fatica di leghe leggere in presenza di intagli. *Degree Thesis*, University of Padova (in Italian).
- Lukas, P., Kunz, L., Weiss, B., Stickler, R.** (1986): Non-damaging notches in fatigue. *Fatigue Fract Engng Mater Struct* 9, pp. 195-204.
- Neuber, H.** (1936). *Forschg Ing-Wes* 7, pp. 271-281.
- Neuber, H.** (1958): Theory of notch stresses: principles for exact calculation of strength with reference to structural form and material. Springer Verlag, Berlin, Germany.
- Nisitani, H., Endo, M.** (1988): Unified treatment

of Deep and Shallow Notches in Rotating Bending. In: *Basic questions in fatigue* Vol. 1, ASTM STP 924, J. T. Fong and R. J. Fields, Editors, pp. 136-153.

Peterson, R. E. (1959) Notch Sensitivity. In: *Metal Fatigue*, Sines G., Waisman J. L., Editors. New York. McGraw Hill, pp. 293-306.

Susmel, L. (2004) A unifying approach to estimate the high-cycle fatigue strength of notched components subjected to both uniaxial and multi-axial cyclic loadings. *Fatigue Fract Engng Mater Struct* 27, pp. 391-411.

Susmel, L., Taylor, D. (2003): Fatigue Design in the Presence of Stress Concentrations. *Int J of Strain Analysis for Engng Comp* 38, pp. 443-452.

Susmel, L., Taylor, D. (2006) A simplified approach to apply the theory of critical distances to notched components under torsional fatigue loading. *Int. J. Fatigue* 28, pp. 417-430.

Susmel, L., Taylor, D. (2003) Two methods for predicting the multiaxial fatigue limits of sharp notches. *Fatigue Fract Engng Mater Struct* 26, pp. 821-833.

Susmel, L., Taylor, D. (2006) Can the conventional High-Cycle Multiaxial Fatigue Criteria be re-interpreted in terms of the Theory of Critical Distances? *Structural Durability & Health Monitoring* 2 (2), pp. 91-108.

Susmel, L., Taylor, D. (2007) A novel formulation of the Theory of Critical Distances to estimate Lifetime of Notched Components in the Medium-Cycle Fatigue Regime. *Fatigue Fract Engng Mater Struct* 30, pp. 567-581.

Tanaka, K. (1983): Engineering formulae for fatigue strength reduction due to crack-like notches. *Int. J Fracture* 22, pp. R39-R45.

Tanaka, K., Akiniwa, Y. (1987): Notch geometry effect on propagation threshold of short fatigue cracks in notched components. *Fatigue '87*, Vol. II, Edited by R. O. Ritchie and E. A. Starke Jr., 3rd Int. Conf. On Fatigue and Fracture Thresholds, Charlottesville, VA, pp. 739-748.

Tanaka, K., Nakai, Y. (1983): Propagation and non-propagation of short fatigue cracks at a sharp notch. *Fatigue Fract Engng Mater Struct.* 6, pp.

315-327.

Taylor, D. (1999): Geometrical effects in fatigue: a unifying theoretical model. *Int. J. Fatigue* 21, pp. 413-420.

Taylor, D. (2001): A mechanistic approach to critical-distance methods in notch fatigue. *Fatigue Fract Engng Mater Struct* 24, pp. 215-224.

Taylor, D., Barrett, N., Lucano, G. (2002): Some new methods for predicting fatigue in welded joints. *Int J Fatigue* 24, pp. 509-518.

Taylor, D., Bologna, P., Bel Knani, K. (2000): Prediction of fatigue failure location on a component using a critical distance method. *Int J Fatigue* 22, pp. 735-742.

Taylor, D., Hughes M. and Allen D. (1996): Notch fatigue behaviour in cast irons explained using a fracture mechanics approach. *Int J Fatigue* 18, pp. 439-445.

Taylor, D, Wang, G. (2000): The validation of some methods of notch fatigue analysis. *Fatigue Fract Engng Mater Struct* 23, pp. 387-394.

Usami, S. (1987): Short Crack Fatigue Properties and Component Life Estimation, In: *Current Research on Fatigue Cracks* Vol. I, Elsevier Applied Science, pp. 119-147.

Williams, M. L. (1952): Stress singularities resulting from various boundary conditions in angular corners of plates in extension. *J Appl Mechanics* 19, pp. 526-528.

Yates, J. R., Brown, M. W. (1987): Prediction of the length of non-propagating fatigue cracks. *Fatigue Fract Engng Mater Struct* 10, pp. 187-201.